IET Image Processing

Case Study

IET Journals
The Institution of Engineering and Technology

Fuzzy enhanced image fusion using pixel intensity control

ISSN 1751-9659
Received on 29th May 2017
Revised 27th August 2017
Accepted on 1st October 2017
E-First on 20th December 2017
doi: 10.1049/iet-ipr.2017.0405
www.ietdl.org

Amita Nandal[1], *Vidhyacharan Bhaskar*[2] ✉

[1]*University of Information Science and Technology, Ohrid, Macedonia*
[2]*Department of Electrical and Computer Engineering, San Francisco State University, 1600 Holloway Avenue, San Francisco, CA 94132, USA*
✉ *E-mail: vcharan@gmail.com*

Abstract: This study is based on improving the visual quality of the images captured under different illumination conditions, i.e. overexposed and underexposed. This study presents a fuzzy image enhancement process based on a finite fuzzy set which is defined to optimise entropy, noise, intensity and edge information. In the proposed fuzzy approach, the overexposed and underexposed images are mapped to form a fuzzy set using membership functions. In the fuzzification process, the degree of belonging of each input to an appropriate fuzzy membership is calculated with respect to intensity, entropy, edge information and background noise. Therefore, the proposed method preserves the details of the image. Indeed, the fuzzy systems are well suited to model the uncertainty that occurs when conflicting operations are performed. Some effective approaches can enhance the image data without increasing noise. However, their ability to reduce the noise during the sharpening process is limited. The proposed method enhances the image by controlling sharpness parameter which affects the visual quality of the image. Both qualitative and quantitative assessments are performed to evaluate the performance of the proposed algorithm.

1 Introduction

Image fusion results in a single image by combining two or more images [1]. The objective of the fusion process is to reduce the uncertainty and to maximise information relevant to a particular application. The major issue in the enhancement of images is noise which is introduced during the sharpening process [2]. Image fusion techniques are widely used in the field of medical applications, remote sensing, military applications, automated surveillance, motion-based recognition, vehicle navigation, human–computer interaction, and video content analysis. A lot of research is focused on developing various tracking algorithms [3–5]. In this study, the proposed work is focused on the fusion of underexposed and overexposed images. The overexposed images suffer from motion blur and underexposed images suffer from noise. The fusion process should preserve the sharpness of edges, contrast, intensity and reduce background noise. Thus, the proposed method uses fuzzy-based image enhancement to improve the visibility of underexposed and overexposed images. In fuzzy set modelling, by using an iterative process, noise can be progressively reduced by setting an appropriate value of sharpness parameter. The performance of the image fusion algorithm depends on the right intensity fusion of registered images. The main objective of image enhancement is to process the image so that the result is more suitable than the original image for a specific application using transform domain and special domain methods [6–9]. Pixel-based contrast enhancement is one of the important image enhancement techniques in the spatial domain. There are various methods used in the literature, such as discrete wavelet transform (DWT)-based image fusion [10], DWT with gamma enhancement [11], DWT with histogram equalisation (HE) [12], contrast enhancement using gamma correction (GC) along with weighted distribution [13] and directional contrast-based enhancement using fuzzy transform enhancement [14] which is written as directional contrast-fuzzy transform (DC-FTR) throughout this paper.

In the DWT-based image fusion, the key step is to define a fusion rule to create a new composite representation [10]. This simple scheme provides just the absolute wavelet coefficients that exist at the same location in input images as it exists at the location in the fused image. However, as we know that the noise and artefacts usually have higher salient features in the image; therefore, this method is sensitive to noise and artefacts. In [11], image enhancement using GC is used to reduce the Gaussian noise present in images. GC has been applied to enhance smaller details, texture and contrast of the images, but it has blurring effects after filtration. This is removed in the proposed method by using the parameter for intensity control of pixels. Another method that performs a cumulative sum of normalised histogram values result in an image with a uniform distribution of intensities, high contrast, and increased dynamic range and this method is known as histogram equalization (HE) [12]. In [13], an automatic transformation technique that improves the brightness of dimmed images via GC and the probability distribution of luminance pixels is presented. However, because of modified sub-histograms used in this method, it might lose some statistical information which might reduce the effect of enhancement. It is based on non-linear transformation which maps the pixel intensity of the input image to the pixel intensity in the output image. Another novel image fusion algorithm based on the directional contrast in the fuzzy transform (FTR) domain is described in [14] where input images to be fused are first divided into several non-overlapping blocks. The components of these sub-blocks are fused using directional contrast based fuzzy fusion rules in the FTR domain. The fused sub-blocks are then transformed into original size blocks using inverse-FTR. However, this method does not deal with the noise minimisation. It incorporates contrast improvement using the maxima fuzzy rule. There are various fuzzy membership functions and statistics in the literature that can be used to improve the fused image quality [15–17]. The proposed algorithm uses the fuzzy set having four components which yield better image and are based on maximising pixel intensity, maximising entropy, maximising edge information and minimising background noise to enhance the output image.

The rest of the paper is organised as follows: Section 2 describes the fuzzy transformation concept. Section 3 presents details of the proposed fusion method. Various performance measures are discussed in Section 4. Section 5 provides the numerical results and discussions. Finally, Section 6 presents the conclusion.

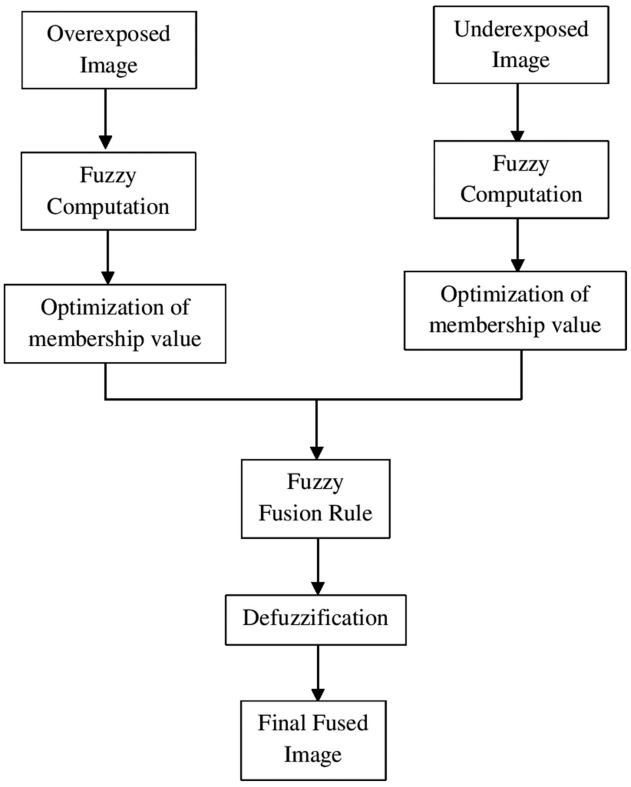

Fig. 1 *Block diagram of proposed fusion methodology*

2 Fuzzy transformation

By using the definition of fuzzy sets [18, 19] an image of size $M \times N$ with intensity levels $(0 \text{ to } L-1)$ is denoted as fuzzy singletons in fuzzy sets connecting with pixel intensity values of the image. In this study, the normalised fuzzy set $\mu(i, j)$ is divided into four regions as average contrast $(\mu_{\text{avg}}(i, j))$, maximum entropy $(\mu_{\text{entropy}}(i, j))$, maximum edge information $(\mu_{\text{edgeinfo}}(i, j))$ and minimum background noise $(\mu_{\text{bnoise}}(i, j))$. Here $i = 1, 2, 3, \ldots, M$ and $j = 0, 1, 2, \ldots, N$. These functions are described later in the paper. The choice of multiple membership functions for these fuzzy sets leads to the improved quality of the fused image. In this study, we have used the Gaussian membership function of the fuzzy sets with specified fuzzy rules. The basic concept of the fuzzy logic is extended in the proposed method where the fuzzy sets are based on the fuzzy rule, which is useful for process simulation, image diagnosis, decision support and process control. The main concern in the fuzzy system is the generation of the membership function with a set of fuzzy rules. A fuzzy system is developed by a set of fuzzy rules with multiple input and output. The membership function of fuzzy sets can be trapezoidal, triangular, sigmoid or Gaussian [20]. In this study, fuzzy image fusion is applied to produce more informative images using the Gaussian membership function.

3 Proposed method

In this work, image enhancement has been discussed by defining fuzzy sets whose parameters are found by optimisation of entropy and other visual factors using the fuzzy logic. In our work, images to be fused are captured under different illumination conditions, i.e. under insufficient illumination (known as underexposed images $(I_{\text{u}}(i, j))$ and images captured with too much of light (known as overexposed images and underexposed image $(I_{\text{o}}(i, j))$). The block diagram of the proposed method is shown in Fig. 1. The proposed method has four stages of steps:

i. In the first stage, fuzzy image transformation for underexposed and overexposed image fusion, we can perform normalisation of intensity distribution from the images of the same scene.
ii. In the second stage, a fuzzy computation is used to evaluate the fuzzy membership function of transformed images.
iii. The next stage is to integrate overexposed and underexposed images using the fuzzy fusion rule with an optimised fuzzy membership value.
iv. Finally, the proposed fuzzy image fusion method uses the most selected membership value and associated information by fuzziness to fuse overexposed and underexposed images while preserving as much as information as possible.

3.1 Construction of proposed Gaussian membership functions

A technique of extracting the fuzzy rules and calculating parameters of the fuzzy set is described in [21]. Consider a fuzzy set where $\boldsymbol{I}_l^p$ is the input vector and $\boldsymbol{O}_l^q$ is the output vector, such that l is the size of the fuzzy vector. p is the length of the input vector, $p = \{1, 2, \ldots, m_1\}$ and q is the length of the output vector, $q = \{1, 2, \ldots, n_1\}$. Let $X = \{x_1, \ldots, x_n\}$ is the initial set of elements. The fuzzy membership of X is defined as $\mu_T(x_i, x_j) \in \{0, 1\}, \forall\, x_i, x_j \in X$. Here, $T: X \times X \to [0, 1]$. Using fuzzy level α the membership is defined as

$$\mu_l = \begin{cases} \mu_{A^l}(x_i), & x_i \in \boldsymbol{A}_\alpha^l, \\ 0, & \text{otherwise}. \end{cases} \tag{1}$$

$\boldsymbol{A}_\alpha^l = \{A^1, \ldots, A^n\}$ is the fuzzy matrix of the fuzzy set on X, where $l = \{1, 2, \ldots, n\}$.

Now let us consider m_l^t and σ_l^t are the members of the Gaussian fuzzy set. $F \in \{m_l^t, \sigma_l^t\}$, $t = 1, \ldots, m_1$ and $l = 1, \ldots, n_1$. In general, the Gaussian membership function $(\mu(F))$ is written as

$$\mu(F) = \exp\left[\frac{-(1/2)(x^t - m_l^t)}{\sigma_l^t}\right], \quad -\infty < x^t < \infty. \tag{2}$$

Here m_l^t denotes the membership centre and σ_l^t represents the Gaussian mean function spread. We can represent the spread for left and right side as

$$[\sigma_l^t]_{\text{left}} = \frac{x_{\min}^t - m_l^t}{\sqrt{2\ln(1-\alpha)}} \text{ and } [\sigma_l^t]_{\text{right}} = \frac{x_{\max}^t - m_l^t}{\sqrt{2\ln(1-\alpha)}},$$

respectively. Here α is the level of the fuzzy set. This fuzzy membership function is also plotted later.

In the proposed fuzzy approach, we map multiple inputs from the two sets of images, i.e. overexposed and underexposed images to a single set of output. The inputs are first converted into a set of predefined membership functions. That is how the set of membership functions is first defined. A fuzzy membership function is a set of data Z, which can be defined as mapping $Z \to [0, 1]$. We have used the grey scale pixel values from [0–255] in four regions as average contrast, maximum entropy, edge information, and background noise. The underexposed and overexposed images are enhanced using the fuzzy image enhancement process based on the Gaussian membership function. If the image edge is deteriorated due to noise, it can be improved by fuzziness. The edge regions of the image are different from the other regions due to ordered, structural and directive characters [22, 23]. For edge detection, the threshold property can also be used [24]. In this study, we have used the fuzzy theory for image fusion which combines the edge information. The non-linear fuzzy enhancement for edge regions is applied to the grey image. Then, information measure entropy based on edge points and noisy points is considered. This non-linear membership function is specified in terms of $\mu(F)$ from (1) as

$$F_{\text{E}}(i, j) = \frac{1}{1 + \mu(F)\left|\alpha(x(i, j) - \bar{x}(i, j))\right|}. \tag{3}$$

$x(i, j)$ is the grey value of the pixel, $\bar{x}(i, j)$ is the mean value of the pixel, α is the fuzzy level such that $\alpha(x(i, j) - \bar{x}(i, j))$ is in the range $(-0.5, 0.5)$. To enhance the edge details of the image, a non-linear mapping from a grey space to a fuzzy space is applied to strengthen a weak edge. The membership function reflects the degree of membership between the centre pixel and its region. If the difference is small, then it depicts a large degree [24, 25]. The grey value is transformed into the fuzzy eigen space by applying a fuzzy transform to each pixel.

Let us consider that the image region is divided into strong (S) and weak (W) intensity regions based on intensity threshold (τ). We can consider the probability function in the form of the intensity histogram of the input image. Let h_i is the probability of the ith histogram bin. Then the cumulative probability is $P_\tau = \sum_{i=1}^{N_\tau} h_i$. Here, N_τ is the number of histogram bins with intensity values less than or equal to threshold τ. Now we can write the strong and weak intensity pixels based on the intensity threshold as $S(i, j)$ and $W(i, j)$, respectively, such that $S(i, j) = \begin{cases} 1, & h_i \le \tau \\ 0, & \text{otherwise} \end{cases}$ and $W(i, j) = 1 - S(i, j)$.

The entropy function can be written as

$$E(S(i, j)) = \ln P_\tau - \frac{1}{P_\tau} \sum_{i=0}^{N_\tau} h_i \ln h_i, \tag{4a}$$

$$E(W(i, j)) = \ln(1 - P_\tau) - \frac{1}{(1 - P_\tau)} \sum_{i=N_\tau+1}^{H} h_i \ln h_i, \tag{4b}$$

where H is the total number of histogram bins. The threshold (τ) determines the boundary condition between the noise and information content of the image. The threshold is represented as $\tau = \arg\max \{E(S(i, j)) + E(W(i, j))\}$. Using (4a) and (4b) the entropy-based membership function is represented as

$$F_{\text{En}}(i, j) = E(S(i, j)) + E(W(i, j)). \tag{5}$$

The optimum threshold is determined by maximising the sum of entropies [20, 26] for strong and weak regions. Suppose τ_η is the noise threshold where η is the noise level and τ is the intensity threshold. The membership function for strong and weak regions is written for intensity and noise threshold as

$$\mu_{\text{S}}(i, j) = \max \left\{ \min \left(-(x(i, j) - \tau)/(\tau - \tau_\eta), 1\right), 0 \right\}, \tag{6a}$$

$$\mu_{\text{W}}(i, j) = 1 - \mu_{\text{S}}(i, j), \tag{6b}$$

where $x(i, j)$ is the pixel value at space (i, j). In the fuzzification process, each strong and weak input pixel is represented by membership values $\mu_{\text{S}}(i, j)$ and $\mu_{\text{W}}(i, j)$, respectively. These membership values are combined using the fuzzy rule. Let us assume m is a fused membership value. When one membership value is associated with strong and weak regions then m is enhanced. When the membership value originates from the noise we suppress it. To enhance the degree of membership of m the fuzzy operator is written as

$$m = \begin{cases} \mu_{\text{S}} + \mu_{\text{W}} - \mu_{\text{S}}\mu_{\text{W}}, & \text{for strong region,} \\ 1 - \sqrt{(1 - \mu_{\text{S}})(1 - \mu_{\text{W}})}, & \text{for weak region.} \end{cases} \tag{7}$$

The fused degree of membership is written in pixel intensity as $\eta + (I_{\max} - \eta)m$, if $m > 0$ and $I_{\text{F}} = \begin{cases} \eta_m, & \text{if } m > 0 \\ \eta(1 - m), & \text{otherwise} \end{cases}$. Here, $I_{\max}$ is the maximum grey value and I_{F} is the fused intensity value.

The fuzzy operator is used to enhance the performance of the image [26]. It is represented as (G) such that

$$G = \sum_{i,k=1}^{M} \sum_{j,l=1}^{N} \frac{1}{d(i, j) + 1} (1 - \mu(F))^m \| x(i, j) - c(k, l) \|^2, \tag{8}$$

where $d(i, j)$ is the distance between two nearby high intensity pixels. G is a control parameter which controls the trade-off between image noise and image details. Our aim is to converge noisy pixels and non-noisy pixels. We will use the fuzzy membership function to suppress the influence of noise described in [24]. By using the definition of G we can write the objective function $\sum_{i,k=1}^{M} \sum_{j,l=1}^{N} \left[(\mu(F))^m || x(i, j) - c(k, l) ||^2 + G\right]$ using the fuzzy membership for two-dimensional images, where $F \to (i, j)$, such that $\mu(F) \to \mu(i, j)$. We can write the fuzzy membership values as (see equation below) Here

$$c(k, l) = \frac{\sum_{i,k=1}^{M} \sum_{j,l=1}^{N} \mu(k, l)^m x(i, j)}{\sum_{i=1}^{M} \sum_{j=1}^{N} \mu(i, j)^m}.$$

Now we highlight the importance of the accurate estimation of the fuzzy factor to suppress the influence of noisy pixels. The coefficient of variation is $\mathscr{C}(i, j) = \left((\text{var}(x(i, j)))/(\bar{x}(i, j))^2\right)$. $\text{var}(x(i, j))$ is the intensity variance for pixel $x(i, j)$ and $\bar{x}(i, j)$ is the mean of the image. $\mathscr{C}(i, j)$ is the coefficient of variation, which is the measure of the homogeneity degree in grey values. It means that a high value of this coefficient has more influence on noise and a low value signifies low influence on noise. Based on this coefficient, the new fuzzy factor can be written as

$$G'(k, l) = \begin{cases} \sum^{\left(1/\left(2 + \min\left[\mathscr{C}^2(i, j), \mathscr{C}^2(k, l)\right]\right)\right)} \cdot (1 - \mu(F))^m || x(i, j) - c(k, l) ||^2, \\ \qquad \text{if } \mathscr{C}(i, j) \ge \mathscr{C}(k, l), \\ \sum^{\left(1/\left(2 - \min\left[\mathscr{C}^2(i, j), \mathscr{C}^2(k, l)\right]\right)\right)} \cdot (1 - \mu(F))^m || x(i, j) - c(k, l) ||^2, \\ \qquad \text{if } \mathscr{C}(i, j) \le \mathscr{C}(k, l). \end{cases} \tag{9}$$

$\mathscr{C}(i, j)$ is the coefficient of variation in the pixel at (i, j), which can be treated as a reference pixel. $\mathscr{C}(k, l)$ is the coefficient of variation in the neighbouring pixel at (k, l) which is the variation from the central pixel space. $G'(k, l)$ balances the membership value of the central pixel by taking into account the coefficient of variation as well as the grey value of neighbouring pixels. Therefore, the noise-based fuzzy membership function becomes

$$F_N(i, j) = \sum_{i,k=1}^{M} \sum_{j,l=1}^{N} (\mu(F))^m || x(i, j) - c(k, l) ||^2 + G'. \tag{10}$$

3.2 Image fusion algorithm

The proposed algorithm uses a fuzzy logic based on pixel intensity, entropy, edge information and background noise to enhance the output image. It has the following steps:

Step 1: calculate the optimised contrast value of each input pixel

$$x_{\text{opt}}(i, j) = \frac{(x(i, j) - x_{\min})}{(x_{\max} - x_{\min})}. \tag{11}$$

$$\frac{1}{\sum_{i,k=1}^{M} \sum_{j,l=1}^{N} \left(\left(|| x(i, j) - c(k, l) ||^2 + G(k, l)\right)/\left(|| x(i, j) - c(k, l) ||^2 + G(i, j)\right)\right)^{1/(m-1)}}.$$

Here, x_{max} and x_{min} are the maximum and minimum contrast of pixels, where $x(i, j)$ is the absolute value of the image gradient taken as a simple indicator of the image contrast.

Step 2: the image statistics follows Gaussian distribution [19, 20]. Therefore, we can model the membership function for the region of maximum pixel intensity, maximum edge information, maximum entropy, and minimum background noise fuzzy using (2), (3), (5) and (10), respectively, as

$$\mu_{avg} = \frac{(1 + (x_{min}/x_{max}))}{2(1 - (x_{min}/x_{max}))}\mu(F), \tag{12a}$$

$$\mu_{edgeinfo} = \sum_{i=1}^{M}\sum_{j=1}^{N} e^{\left(\left(-(x_{opt(i,j)} - x(i,j))^2\right)/(2\sigma_{min}^2)\right)}F_E(i, j), \tag{12b}$$

$$\mu_{entropy} = \sum_{i=1}^{M}\sum_{j=1}^{N} \frac{\log_2(x(i,j)_{max})}{\log_2(x(i,j)_{min})}F_{En}(i, j), \tag{12c}$$

$$\mu_{bnoise} = \sum_{i=1}^{M}\sum_{j=1}^{N} e^{\left(\left(-(x_{opt(i,j)})^2\right)/(2\sigma_{min}^2)\right)}F_N(i, j), \tag{12d}$$

where σ is chosen as the standard deviation (SD) from the fuzzy set.

Step 3: the fuzzified images with respective regions are derived. The notation $f_{avg}(i, j)$ represents the average contrast-based fuzzified region. The fuzzification of the image is done using the following steps:

1. If $0 < x_{opt(i,j)} < \mu_{avg}$, then $f_{avg}(i, j) = \left(\left(x_{opt}^{2^m}(i, j)\right)/(1 - \mu_{avg})^{2^{m-1}}\right)$,
2. If $0 < x_{opt(i,j)} < \mu_{edgeinfo}$, then $f_{edgeinfo}(i, j) = \left(\left(x_{opt}^{2^m}(i, j)\right)/(1 - \mu_{edgeinfo})^{2^{m-1}}\right)$,
3. If $0 < x_{opt(i,j)} < \mu_{entropy}$, then $f_{entropy}(i, j) = \left(\left(x_{opt}^{2^m}(i, j)\right)/(1 - \mu_{entropy})^{2^{m-1}}\right)$,
4. If $0 < x_{opt(i,j)} < \mu_{bnoise}$, then $f_{bnoise}(i, j) = \left(\left(x_{opt}^{2^m}(i, j)\right)/(1 - \mu_{bnoise})^{2^{m-1}}\right)$,
5. else if
6. $\mu_{avg} - x_{opt(i,j)} < 1$, then $f_{avg}(i, j) = 1 - \left(\left(x_{opt}^{2^m}(i, j)\right)/\left(1 - \mu_{avg}\right)^m\right)$,
7. $\mu_{edgeinfo} - x_{opt(i,j)} < 1$, then $f_{edgeinfo}(i, j) = 1 - \left(\left(x_{opt}^{2^m}(i, j)\right)/\left(1 - \mu_{edgeinfo}\right)^{2^{(m-1)}}\right)$,
8. $\mu_{entropy} - x_{opt(i,j)} < 1$, then $f_{entropy}(i, j) = 1 - \left(\left(x_{opt}^{2^m}(i, j)\right)/\left(1 - \mu_{entropy}\right)^{2^{(m-1)}}\right)$,
9. $\mu_{bnoise} - x_{opt(i,j)} < 1$, then $f_{bnoise}(i, j) = 1 - \left(\left(x_{opt}^{2^m}(i, j)\right)/(1 - \mu_{bnoise})^{2^{(m-1)}}\right)$.

Now, pixel-wise addition is performed to obtain the fuzzified image as

$$f_{img}(i, j) = \sum_{i=1}^{M}\sum_{j=1}^{N} f_{avg}(i, j) + f_{entropy}(i, j) + f_{edgeinfo}(i, j) - f_{bnoise}(i, j), \tag{13}$$

where $f_{img}(i, j)$ is the fuzzified image.

Step 4: the defuzzified image ($df_{img}(i, j)$) with GC is obtained using

$$df_{img}(i, j) = f_{img}(i, j)^{\gamma}. \tag{14}$$

Here, γ is a non-linear relationship between intensity and pixel values. The mean for the fused image is higher than the overexposed and underexposed images, and similarly, the variance is lower because it is observed that the gamma corrected image is lighter than the original image for $\gamma < 1$, and is darker than the original image for $\gamma > 1$.

3.3 Normalisation of images under different illumination

There are various methods in the literature that describe illumination-based normalisation [27, 28]. The proposed algorithm is focused on the extraction of fuzzy multiple illumination features from the underexposed and overexposed images. The visual recovery is better using the proposed method because the spatial structure is preserved which makes the performance of the proposed algorithm satisfactory. We have considered both small-scale and large-scale features in the normalisation process and the synthesised normalised image has better visual quality. The processed small-scale and large-scale image features are combined to generate a normalised image. According to Lambertian reflectance theory [29], the input images $I_o(i, j)$ and $I_u(i, j)$ can be described using the reflectance component and illumination effect due to the different illumination of images which is considered in our experiments which are written as

$$I_o(i, j) = \mathfrak{r}_o(i, j) \cdot \mathfrak{i}_o(i, j), \tag{15a}$$

$$I_u(i, j) = \mathfrak{r}_u(i, j) \cdot \mathfrak{i}_u(i, j). \tag{15b}$$

The subscript o and u denote the overexposed and underexposed image, respectively. $\mathfrak{r}$ is the reflectance component and $\mathfrak{i}$ is the illumination component. Both of these components are dependent on the illumination of overexposed and underexposed images. The overexposed image has a higher value of the illumination component while the underexposed image has a higher value of the reflectance component. In the literature, there were few methods proposed to extract these components but it is still in infancy [29, 30]. The fuzzified image after normalisation can be written in the form of the average of the reflectance and illumination components of overexposed and underexposed images as

$$f_{img}(i, j) = \left\{\frac{\mathfrak{r}_o(i, j) + \mathfrak{r}_u(i, j)}{2}\right\}\left\{\frac{\mathfrak{i}_o(i, j)(i, j) + \mathfrak{i}_u(i, j)}{2}\right\}. \tag{16}$$

$f_{img}(i, j)$ can be written as

$$f_{img}(i, j) = \{\mathfrak{r}\}\{\mathfrak{i}\}. \tag{17}$$

Here, $\mathfrak{r} = ((\mathfrak{r}_o(i, j) + \mathfrak{r}_u(i, j))/2)$ and $\mathfrak{i} = ((\mathfrak{i}_o(i, j)(i, j) + \mathfrak{i}_u(i, j))/2)$.

Taking the logarithm on both sides in (17) we get

$$\log\left(f_{img}(i, j)\right) = \log(\mathfrak{r}) + \log(\mathfrak{i}). \tag{18}$$

The logarithm of luminance is the accurate approximation of brightness and it can reduce the effect of over-illumination and reflectance from the overexposed and underexposed images, respectively. The solution of (18) is computed to get the values of $\hat{\mathfrak{r}}$ and $\hat{\mathfrak{i}}$ as edge-preserving capability using the approach given in [30]. Mathematically

$$\hat{\mathfrak{r}} = \arg\min\left\{\int|\nabla\mathfrak{r}| + \lambda\,||f_{img}(i, j) - \mathfrak{r}||_{L^{-1}}\right\}, \tag{19a}$$

$$\hat{\mathfrak{i}} = f_{img}(i, j) - \hat{\mathfrak{r}}. \tag{19b}$$

$\int|\nabla\mathfrak{r}|$ is the total variation in reflectance and $||\,.\,||_{L^{-1}}$ is the L-norm. λ is the scalar constant whose value lies between [0, 1] which is based on image size [31]. For small size images, the value of λ is considered in the range of $0 < \lambda < 0.4$ and for larger size images the value of λ is taken in the range of $0.4 < \lambda < 1$. For our experiments, we have considered the value of λ as 0.4 for image size of 512×512. By minimising the value of $\int|\nabla\mathfrak{r}|$ and $||f_{img}(i, j) - \mathfrak{r}||_{L^{-1}}$ the normalised approximation based on image size is obtained.

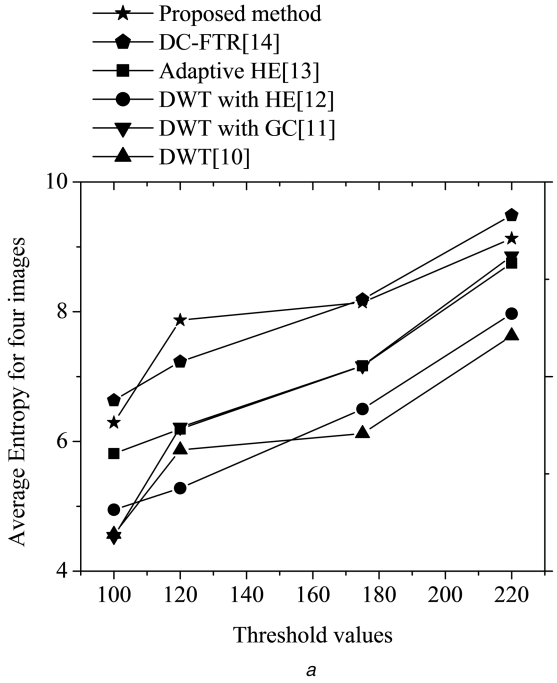

Fig. 2 *Quantitative comparison of performance measures*
(a) Plot showing variation of average entropy w.r.t. threshold (τ) for final fused image,
(b) Plot showing variation of average SD w.r.t. threshold (τ) for final fused image

In the proposed technique, optimisation of contrast, entropy, background noise and edge information is achieved globally using fuzzification. It has been observed that entropy reduces with enhancement. The fuzzy set is defined and values are evaluated automatically for the input image by optimising contrast and entropy in the fuzzy domain. However, the membership function is evaluated by maximising fuzzy contrast, which is cumulative fuzzy variance about the SD. Detailed results have been discussed in the subsequent section. We have considered four image sets, i.e., Bowl, Room, Cup and Bridge for the demonstration. A clear improvement is observed as far as the restorations of image details are concerned.

4 Performance measures

The popular metrics like entropy, SD, root mean square error (RMSE), average gradient (AG), fusion loss (FL), fusion artefacts, quality distortion index, fuzzy density, computational time, and correlation coefficient are accessed for performance evaluation of the proposed fusion method. Initially, we have selected the overexposed and underexposed images of 512×512 pixel size and the grey scale map has 256 grey levels. All the images are of the same size and lie in the visible light band [32]. Simulations are performed on MATLAB 2013a on a PC with Intel Core i5/2,67 GHz/4 GB processor.

Entropy (E) is the information content of the image and it is represented as

$$E = -\sum_{i=0}^{L-1} D_i \log_2 D_i . \tag{20}$$

Here, L is the total of grey levels, $D_i = \{D_0, D_1, \ldots D_{L-1}\}$ is the probability distribution of each level. SD measures the contrast. An image with high contrast will have a high SD. The SD of an image is calculated as

$$\mathrm{SD} = \sqrt{\frac{1}{M \times N} \sum_{i=1}^{M} \sum_{j=1}^{N} (I(i,j) - m(i,j))^2} . \tag{21}$$

Here, the mean is $m(i,j) = (1/(M \times N)) \sum_{i=1}^{M} \sum_{j=1}^{N} f_{\mathrm{img}}(i,j)$. $I(i,j)$ is the average of overexposed ($I_{\mathrm{o}}(i,j)$) and underexposed image ($I_{\mathrm{u}}(i,j)$).

Fig. 2*a* shows the variation of entropy w.r.t. threshold values for the final fused image. We have taken the average entropy of four images in Fig. 2*a*. Fig. 2*a* depicts that the final fused image extracts more information content and results in larger information entropy as compared with overexposed and underexposed images. The entropy content of the final fused image is a result of the maximising entropy of strong and weak regions which is computed using entropy-based membership function in (5). Also, for lower values of intensity threshold, the entropy content is smaller than higher intensity thresholds. The threshold value for the strong region is set as $165 < \tau < 255$ and it is set as $105 < \tau < 165$ for the weak region in our experiments. Fig. 2*b* shows variation of SD w.r.t. threshold values. We have taken the average SD of four images in Fig. 2*b*.

We have observed from our experiments that as the value of threshold increases then the SD decreases as shown in Fig. 2*b*. In our experiments, the value of SD is computed and it is observed that if the closeness between high and low intensity pixels is high, then the SD is also high. The higher value of SD is related to larger variance which causes mean square error to increase. As is clear from Fig. 2*b* the SD reduces when the threshold value increases which in turn improves the image quality. When the intensity threshold is set larger the overall image quality is better because the strong region has a major contribution to larger threshold values.

AG is a parameter which tells the change in the image with respect to edge information. It is a very important parameter for boundary detection specifically. The AG is denoted as g which varies with respect to edge information as $((\partial g)/(\partial f_{\mathrm{edgeinfo}}(i,j)))$

$$\frac{\partial g}{\partial f_{\mathrm{edgeinfo}}} = \frac{\partial \left(f_{\mathrm{img}}(i + \Delta i, j) - f_{\mathrm{img}}(i,j) \right)}{\partial f_{\mathrm{edgeinfo}}(i,j)} . \tag{22}$$

Here Δi is the change in pixel space by a small value which is taken as 1 in our experiments. When we are considering pixel wise computation for the image, the partial derivative will have

$$\frac{\partial g}{\partial f_{\mathrm{edgeinfo}}(i,j)} = \frac{\partial \left(f_{\mathrm{img}}(i+1, j) - f_{\mathrm{img}}(i-1, j) \right)}{2} . \tag{23}$$

Some information of the input image gets necessarily lost in the fusion process which is called as fusion loss (FL). It may affect the performance of certain fusion applications. Mathematically, FL is defined as

$$\mathrm{FL} = \frac{\sum_{i=1}^{M}\sum_{j=1}^{N}\left[\left(1 - f_{\mathrm{img}}(i,j)\right)\right]}{\sum_{i=1}^{M}\sum_{j=1}^{N}\left[I_{\mathrm{o}}(i,j) + I_{u}(i,j)\right]}. \quad (24)$$

Relative global error (RGE) is another important performance measure [24, 33]. This parameter is sensitive to mean shifting. The smaller value of the RGE ensures good image quality. It is calculated as

$$\mathrm{RGE} = \sqrt{\frac{1}{M \times N}\sum_{i=1}^{M}\sum_{j=1}^{N}\left(\frac{\mathrm{RMSE}}{\bar{x}(i,j)}\right)^2}. \quad (25)$$

If the reference image and fused image are alike, the RMSE value equals zero and RMSE will increase when the dissimilarity increases between the fused and reference image which is the average of two images, i.e. underexposed and overexposed.

$$\mathrm{RMSE} = \sqrt{\frac{1}{MN}\sum_{i=1}^{M}\sum_{j=1}^{N}\left(I(i,j) - f_{\mathrm{img}}(i,j)\right)^2}. \quad (26)$$

Using the procedure given in [34], average correlation can be expressed as

$$A_{\mathrm{C}} = \frac{I(i,j) * F(i,j)}{\sqrt{\sum_{i=1}^{M}\sum_{j=1}^{N} I^2(i,j) + F^2(i,j)}}. \quad (27)$$

This measure provides a quantitative measure of the degree of correlation between the two images. When A_{C} is closer to 1, the fusion effect is better.

Image quality index (Q) is used as a measure for image distortion measure. This parameter models image distortion relative to three factors, i.e. loss of correlation, luminance distortion, and constant distortion. We have considered two images, i.e. overexposed and underexposed consisting of different pixel values. The notation d represents the degree of correlation, subscript o and u signify overexposed and underexposed image. The image quality index is calculated as the product of three components. It is represented as

$$Q = \frac{d_{\mathrm{ou}}}{d_{\mathrm{o}}d_{\mathrm{u}}} \cdot \frac{2\bar{d}_{\mathrm{o}}\bar{d}_{\mathrm{u}}}{\bar{d}_{\mathrm{o}}^2 + \bar{d}_{\mathrm{u}}^2} \cdot \frac{2d_{\mathrm{o}}d_{\mathrm{u}}}{d_{\mathrm{o}}^2 + d_{\mathrm{u}}^2}. \quad (28)$$

$$\bar{d}_{\mathrm{o}} = \frac{1}{M \times N}\sum_{i=1}^{M}\sum_{j=1}^{N} I_{\mathrm{o}}(i,j), \quad (29a)$$

$$\bar{d}_{\mathrm{u}} = \frac{1}{M \times N}\sum_{i=1}^{M}\sum_{j=1}^{N} I_{\mathrm{u}}(i,j), \quad (29b)$$

$$d_{\mathrm{ou}} = \frac{1}{M+N-1}\sum_{i=1}^{M}\sum_{j=1}^{N}\left(I_{\mathrm{o}}(i,j) - \bar{d}_{\mathrm{o}}\right)\left(I_{\mathrm{u}}(i,j) - \bar{d}_{\mathrm{u}}\right), \quad (29c)$$

$$d_{\mathrm{u}}^2 = \frac{1}{M+N-1}\sum_{i=1}^{M}\sum_{j=1}^{N}\left(I_{\mathrm{u}}(i,j) - \bar{d}_{\mathrm{u}}\right)^2, \quad (29d)$$

$$d_{\mathrm{o}}^2 = \frac{1}{M+N-1}\sum_{i=1}^{M}\sum_{j=1}^{N}\left(I_{\mathrm{o}}(i,j) - \bar{d}_{\mathrm{o}}\right)^2. \quad (29e)$$

The first component measures the degree of linear correlation between overexposed and underexposed images. It measures the degree of correlation between images. It varies $(-1, 1)$. The second component varies $(0, 1)$ which measures the closeness of the mean luminance between images $I_{\mathrm{u}}(i,j)$ and $I_{\mathrm{o}}(i,j)$. It measures the estimated contrast of images. The third component measures the similarity of contrast between images. It varies $(0, 1)$. The best value of Q is unity.

Peak signal to noise ratio (PSNR) is calculated as

$$\mathrm{PSNR} = 20\log_{10}\left(\frac{L^2}{(1/MN)\sum_{i=1}^{M}\sum_{j=1}^{N}\left(I(i,j) - f_{\mathrm{img}}(i,j)\right)^2}\right), \quad (30)$$

where L in the number of grey levels in the image. It corresponds to the better qualitative image. The PSNR value will be high when the fused and reference images are similar. A higher value implies better fusion.

A fuzzy approach is used to estimate the joint density distribution of the image dataset. The fuzzy density estimation of the output pixel is a probability density function (PDF) represented in terms of the considered image feature [35]. It is calculated as

$$\mathfrak{f}(x) = \frac{1}{M \times N}\sum_{i=1}^{M}\sum_{j=1}^{N}\frac{1}{(2\pi)^{i/2}x(i,j)\det(\boldsymbol{C})^{1/2}} \times \exp\left(\frac{\{x(j,i) - x(i,j)\}^{\mathrm{T}}\boldsymbol{C}^{-1}\{x(i,j) - x(j,i)\}}{2ij}\right). \quad (31)$$

where T denotes the transpose and $\boldsymbol{C}$ is the covariance matrix, which represents the pixel variance among the pixel space(i, j)

$$\boldsymbol{C} = \frac{1}{M \times N}\sum_{i=1}^{M}\sum_{j=1}^{N}\left[x(i,j) - \bar{x}(i,j)\right] - \left[x(i,j) - \bar{x}(i,j)\right]^{\mathrm{T}}. \quad (32)$$

where $\bar{x}(i,j)$ is the mean value of a pixel, which is written as $\bar{x}(i,j) = (1/(M+N))\sum_{i=1}^{M}\sum_{j=1}^{N}x(i,j)$.

The general requirements of an image fusion process include the restoration of all valid and useful pattern information from the source images, while at the same time it should not introduce artefacts that can interfere with the subsequent analysis. The performance measures provide some quantitative comparison among different fusion schemes, mainly aiming at measuring the image definition. Quality refers to both spatial and spectral quality of images. Image fusion methods aim at increasing the spatial resolution of the images while preserving their original spectral content. The spectral content is very important for applications such as photo interpretation and classification that depend on the spectra of objects. The evaluation of the fusion results is based on the quantitative criteria including spectral and spatial properties and definition of images. Numerical statistical parameters are used to quantitatively assess the fused images produced using different fusion algorithms [36–39]. Entropy is an index to evaluate the information content contained in an image. If the value of entropy becomes higher after fusing, it indicates that the information content increases and the fusion performance also improve. Another performance metric is SD, which is more efficient in the absence of noise. It measures the contrast in the fused image. An image with high contrast will have a high SD. RMSE corresponds to pixels in the reference image and the fused image [40, 41]. If the reference image and fused image are alike, the RMSE value equals zero and RMSE will increase when the dissimilarity increases between the reference and fused images. The basic principle of spectral fidelity is that low spatial frequency information in the high-resolution image should not be absorbed in the fusion image so as to preserve the spectral content of the original image. To verify the preservation of spectral characteristics and resolution, fused images are visually compared. The visual appearance may be subjective and depends on a human interpreter.

4.1 Computational complexity analysis

The DWT is one of the most commonly used techniques in image processing [42, 43]. Apart from vector multiplication, the analytical value of DWT has a computational load of $O(4N_t\log_2(N_t)(M+A))$, where N is the number of complex samples produced in t iterations, M is the number of multiplications, and A is the number of additions. This is evident from the computational aspects of the DWT algorithm [44]. In DWT, 2^n scale decomposition is used therefore, the logarithm factor appears in the overall computation cost of the DWT technique. The DWT with GC [11] involves additional

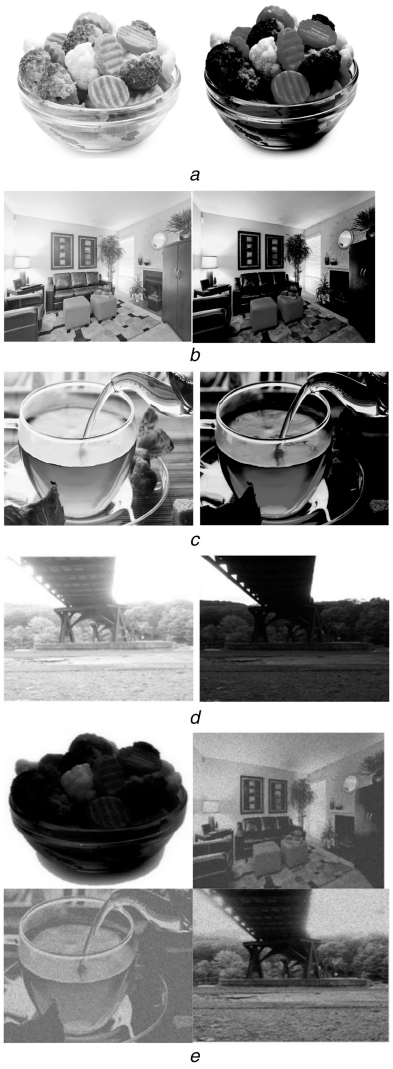

Fig. 3 *Input Images*
(a) Overexposed and underexposed image set 1 (Bowl), ***(b)*** Overexposed and underexposed image set 2 (Room), ***(c)*** Overexposed and underexposed image set 3 (Cup), ***(d)***Overexposed and underexposed image set 4 (Bridge), ***(e)*** DWT [10] based output fused image

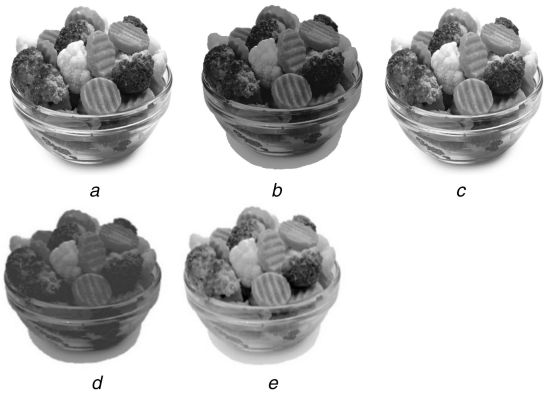

Fig. 4 *Subjective image quality assessment: image set 1 (Bowl)*
(a) DWT with GC fused [11], ***(b)*** DWT with HE fused [12], ***(c)*** Adaptive HE [13], ***(d)*** DC-FTR [14], ***(e)*** Proposed method based

multiplication of N terms for GC. Therefore, the DWT-GC technique has a computational complexity of $O\left(4N_t^2\log_2(N_t)(M+A)\right)$. The DWT with HE [12] includes the computational load of DWT, PDF and cumulative density function (CDF). Therefore, the overall computational complexity of DWT-HE becomes $O\left(N\prod_{i=1}^{p}\mathrm{pr}(i,j)+\mathrm{cd}(i,j)\right)+O(4N_t\log_2(N_t)(M+A))$. Here $\mathrm{pr}(i,j)$ denotes PDF and $\mathrm{cd}(i,j)$ denotes CDF. The adaptive

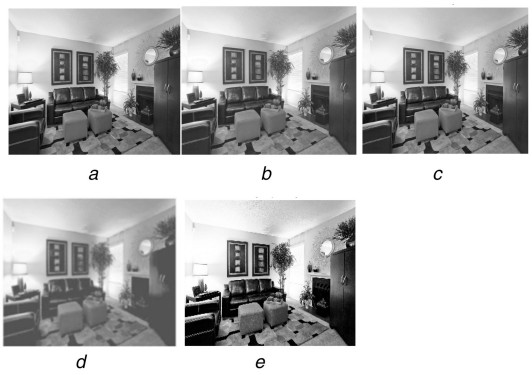

Fig. 5 *Subjective image quality assessment: image set 2 (Room)*
(a) DWT with GC fused [11], ***(b)*** DWT with HE fused [12], ***(c)*** Adaptive HE [13], ***(d)*** DC-FTR [14], ***(e)*** Proposed method based

HE [13] method includes the computational load of DWT, PDF, CDF and a constant. Therefore, the overall computational complexity of adaptive HE becomes $\left(N\prod_{i=1}^{p}\mathrm{pr}(i,j)+\mathrm{cd}(i,j)+\mathbb{k}\right)+O(4N_t\log_2(N_t)(M+A))$. Here, $\mathbb{k}$ is an adaptive constant which varies exponentially w.r.t. the size of the density function under consideration.

For the fuzzy algorithm, the computational complexity is divided into three parts [45, 46], i.e. initialisation, main loop and finalisation. Initialisation and finalisation have a computational complexity of $O(n^p)$, where $n=V_{i=1}^{p}n_i$. We assume that p is the dimension of original partition, n is the number of basic functions, in particular, dimension and N is the number of complex sample points. The main loop will be iterated N times and this loop contains nested loops which are iterated 2^p times, therefore the computational complexity becomes $O(p)$. For the fuzzy partition used in our method, the complexity is $O(p\cdot\log n)$. The computational complexity of the main loop is $O\left(Np+(2^p+\log n)\right)$ for general fuzzy partition [45, 46]. Discrete cosine transform needs $\log_2 N$ stages and each stage involves $N^3/8$ butterflies. So, total $(N^3/8)\log_2 n$ butterflies are computed using fuzzy computation. For DC-FTR [14], the computational complexity includes discrete cosine fuzzy computations which are generalised for fuzzy computation, multiplication and additions as $O(n^p+Np(2^p+\log n)$, $O\left((3/2)N^3\log_2 N\right)$ and $O\left((9/2)N^3\log_2 N-3N^3+3N^2\right)$, respectively. The overall computational complexity becomes $O(n^p+Np(2^p+\log n)+O\left((3/2)N^3\log_2 N\right)+O.$ $\left((9/2)N^3\log_2 N-3N^3+3N^2\right)$

In the proposed algorithm, the computational complexity includes four fuzzy computations related to intensity, entropy, edge information and background noise, which depend on fuzzy partitioning. Finally, the computational complexity including all parts becomes $4\cdot O(n^p+\mathrm{Nr}(2^p+\log n))$. The execution time for various methods is tabulated in experimental results.

5 Numerical results and discussion

The proposed algorithm has been used to enhance the four sets of overexposed and underexposed images, i.e. Bowl, Room, Cup and Bridge of the size 512 × 512 shown in Figs. 3*a–d*, respectively. We have shown the comparison in terms of qualitative measures among DWT-based image fusion [10], DWT with gamma enhancement [11], DWT with HE [12], adaptive HE [13], DC-FTR [14] and the proposed method. The performance of the proposed algorithm is demonstrated using subjective and objective image quality assessment. Fig. 3*e* shows the DWT [10] based output fused image. The DWT method is further improved [11–14], which is evident from the subjective image quality assessment shown in Figs. 4–7 for the four set of images, i.e. Bowl, Room, Cup and Bridge, respectively.

The final image obtained from the fusion methods used in [10–14] can be compared with the proposed method. The proposed

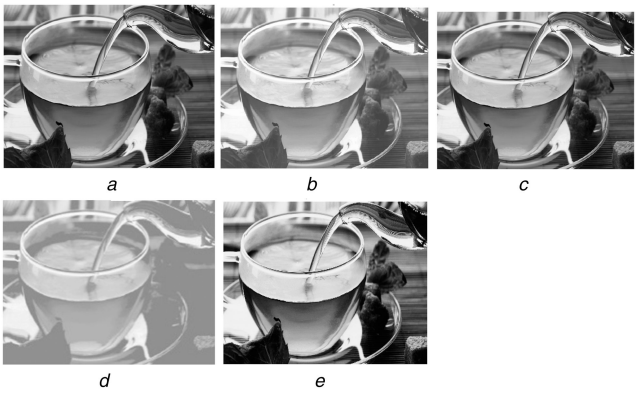

Fig. 6 *Subjective image quality assessment: image 3 (Cup)*
(a) DWT with GC fused [11], ***(b)*** DWT with HE fused [12], ***(c)*** Adaptive HE [13], ***(d)*** DC-FTR [14], ***(e)*** Proposed method based

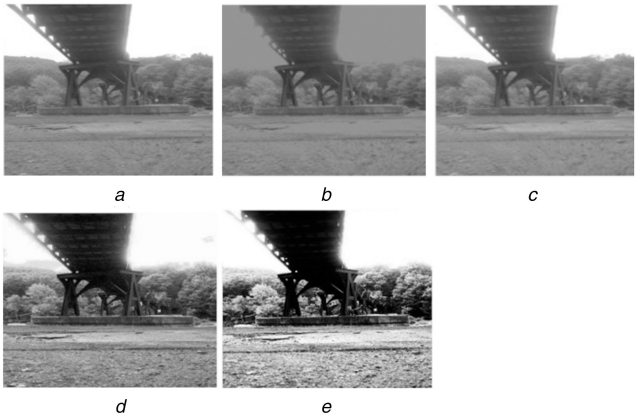

Fig. 7 *Subjective image quality assessment: image 4 (Bridge)*
(a) DWT with GC fused [11], ***(b)*** DWT with HE fused [12], ***(c)*** Adaptive HE [13], ***(d)*** DC-FTR [14], ***(e)*** Proposed method based

method increases the global contrast of images, especially where the image is represented by close contrast values. Through this adjustment, the intensities are better distributed on the histogram, which is clear from the histogram plot. Therefore, the areas of lower local contrast gain higher contrast. The proposed final equalisation accomplishes this by effectively spreading out the most frequent intensity values. Figs. 8*a* and *b* plot the variation in mean and variance, respectively, with variation in gamma from 0.9 to 1.1. This plot is observed for image set 1, i.e. Bowl. Fig. 9*a* plots single membership function. Figs. 9*b–e* show the region plot for $f_{\text{img}}(i, j)$ for image set 1 (Bowl), image set 2 (Room), image set 3 (Cup) and image set 4 (Bridge), respectively. Fig. 10*a* plots four membership functions. Figs. 10*b–e* show the region plot for $f_{\text{img}}(i, j)$ for image set 1 (Bowl), image set 2 (Room), image set 3 (Cup) and image set 4 (Bridge), respectively. It is observed from the region plots that as the number membership functions increase the plot converges better which depicts lower spread in Gaussian membership with less erroneous results.

It is clear from the comparison plots that in the process of fusion, the fusion rule is based on the convergence of strength of source images to avoid the loss of useful information. Comparing with [10–14] the proposed fusion method provides improved visual effects of the fused image and also improves the objective parameter considered as a performance measure in this paper. The entropy and SDs are concerned with the properties of the individual pixels. A large value of entropy ensures a good quality image. SD is an important index to weight the information of the image; it reflects the deviation degree of values relative to the mean of the image. The higher value of SD depicts that the grey grade distribution is more dispersible. High-contrast images correspond to a large SD, and vice versa. AG (g) tells the change in the image with respect to edge information. This parameter tells about the edge information restoration. Some information of the input image gets necessarily lost in the fusion process, which is

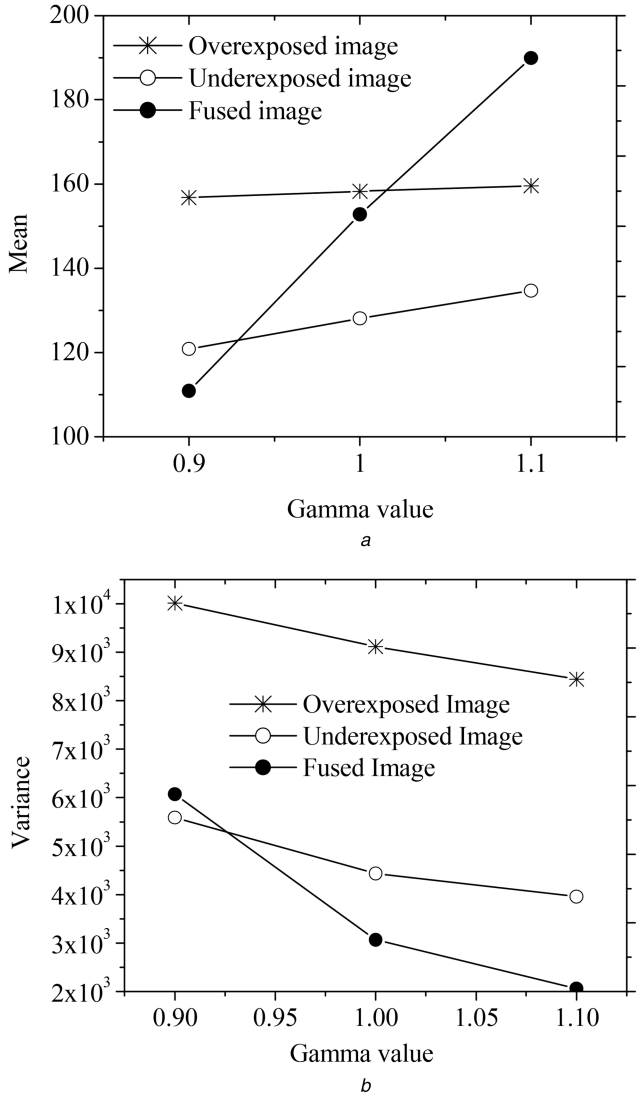

Fig. 8 *Variation in statistical parameters*
(a) Variation in mean with change of gamma values for image set (Bowl), ***(b)*** Variation in variance with change of gamma values for image set (Bowl)

calculated using FL. RGE tells the deviation from the mean value. The degree of correlation between output and input images is calculated using average correlation. The execution time of the various methods is also shown in Tables 1–4. It is observed that the proposed algorithm has lesser execution time in comparison with [10–14]. However, the execution time of the proposed algorithm is comparable to that of the DC-FTR [14] based fusion algorithm.

Tables 1–4 also show a comparison of the quality index performance metric for different fusion methods for $\gamma = 0.2$, 0.4, 0.5, 1 and 1.5. γ is a non-linear relationship between intensity and pixel values. The final fused image is dependent on this parameter as given in (14). The comparison of PSNR performance metric for different fusion methods by varying fuzzy density from 10 to 50% and variance from 0.03 to 0.06. Equation (31) gives the relationship between pixel variance among the pixel space (i, j) and fuzzy density function. PSNR deteriorates for higher values of variance; however, when the fuzzy density is close to 50% the image quality is better than the lower values of fuzzy density. In Table 5, we have shown the execution time with a different membership function, which depicts that as the number of membership functions increases the computational complexity also increases. It is clear from these performance measures that the proposed fusion method has better contrast than the methods used in [10–14]. The quality index for different regions of the fuzzy set w.r.t. $f_{\text{avg}}(i, j)$, $f_{\text{entropy}}(i, j)$, $f_{\text{edgeinfo}}(i, j)$, $f_{\text{bnoise}}(i, j)$ and $f_{\text{img}}(i, j)$ is evaluated in Table 6. It calculates the degree of correlation among images. Equation (28) calculated the quality index. It is analysed

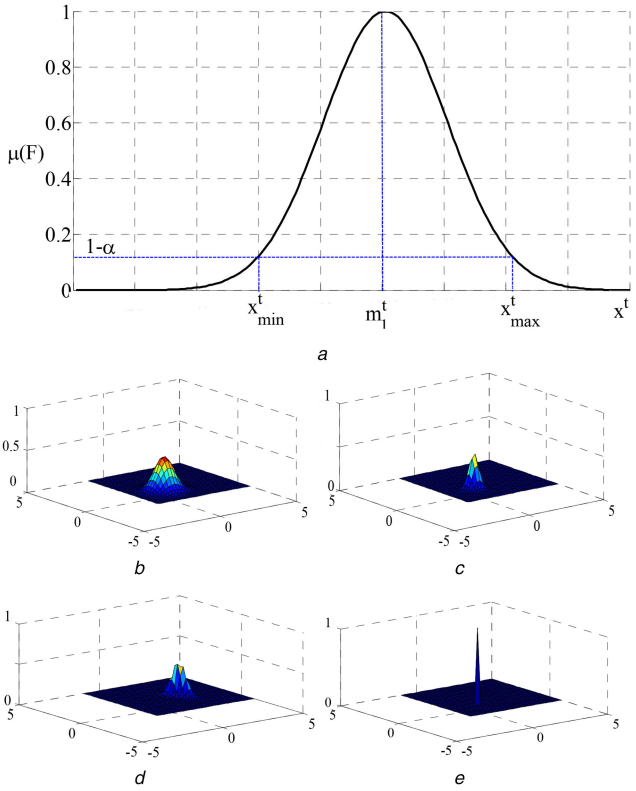

Fig. 9 *Plot considering single membership function based evaluation*

(a) Plot of single membership function, ***(b)*** Region plot for $f_{img}(i, j)$ for image set 1 (Bowl), ***(c)*** Region plot for $f_{img}(i, j)$ for image set 2 (Room), ***(d)*** Region plot for $f_{img}(i, j)$ for image set 3 (Cup), ***(e)*** Region plot for $f_{img}(i, j)$ for image set 4 (Bridge)

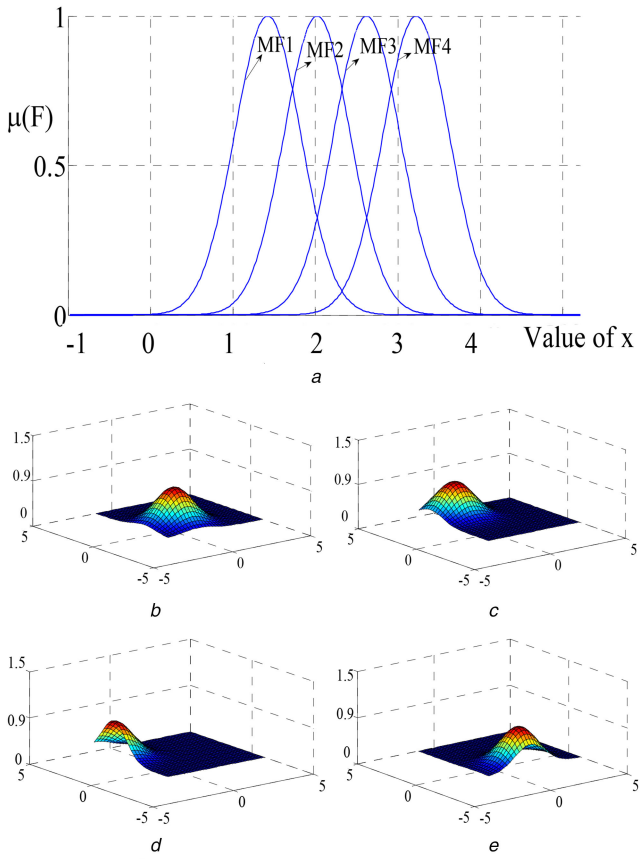

Fig. 10 *Plot considering four membership function based evaluation*

(a) Plot of four membership functions, ***(b)*** Region plot for $f_{img}(i, j)$ for image set 1 (Bowl), ***(c)*** Region plot for $f_{img}(i, j)$ for image set 2 (Room), ***(d)*** Region plot for $f_{img}(i, j)$ for image set 3 (Cup), ***(e)*** Region plot for $f_{img}(i, j)$ for image set 4 (Bridge)

that by involving all four fuzzy regions the quality index improves as compared with quality index involving only one fuzzy region.

Table 7 shows the value of the quality index for the minimised value of $||f_{img}(i, j) - \mathfrak{r}||_{L^{-1}}$ for different image sizes by varying λ.

Table 1 Comparison of various performance metrics for different fusion methods for image set 1 (Bowl)

	Proposed method	DC-FTR [14]	Adaptive HE [13]	DWT with HE [12]	DWT with GC [11]	DWT [10]
entropy	4.997	4.892	4.996	3.984	3.567	3.131
SD	82.558	80.712	79.838	97.569	78.140	99.962
AG	12.685	9.444	7.646	7.774	5.764	5.530
FL	0.016	0.017	0.295	0.049	0.197	0.264
RGE	0.028	0.032	0.034	0.082	0.095	0.097
RMSE	14.380	14.896	17.369	18.935	19.067	21.410
A_C	0.966	0.908	0.891	0.874	0.812	0.801
time, s	8.012	8.367	9.013	8.213	8.556	7.892
			quality index, Q			
$\gamma = 0.2$	0.803	0.628	0.513	0.509	0.803	0.599
$\gamma = 0.4$	0.816	0.609	0.524	0.594	0.814	0.684
$\gamma = 0.5$	0.822	0.589	0.635	0.579	0.825	0.669
$\gamma = 1$	0.832	0.571	0.646	0.565	0.836	0.655
$\gamma = 1.5$	0.901	0.653	0.657	0.551	0.847	0.641
			PSNR for fuzzy density/variance			
0.1/0.06	63.142	62.156	62.172	59.789	56.923	49.156
0.2/0.05	64.291	63.307	63.322	60.944	58.084	50.333
0.3/0.04	66.287	65.303	65.318	62.942	60.081	52.329
0.4/0.03	67.265	66.281	66.296	63.918	61.058	53.307
0.5/0.03	68.043	67.059	67.074	64.696	61.836	54.085

Table 2 Comparison of various performance metrics for different fusion methods for image set 2 (Room)

	Proposed method	DC-FTR [14]	Adaptive HE [13]	DWT with HE [12]	DWT with GC [11]	DWT [10]
entropy	7.822	7.812	7.801	6.605	7.402	5.851
SD	72.779	72.145	72.262	70.385	70.001	74.826
AG	13.023	9.801	8.014	8.141	6.143	5.911
FL	0.016	0.048	0.347	0.122	0.344	0.277
RGE	0.038	0.043	0.046	0.098	0.106	0.107
RMSE	20.126	20.848	24.310	26.501	26.686	29.966
A_C	0.967	0.952	0.871	0.904	0.869	0.862
time, s	9.561	9.650	9.695	9.197	9.140	8.876
			quality index, Q			
$\gamma = 0.2$	0.734	0.473	0.550	0.455	0.632	0.537
$\gamma = 0.4$	0.745	0.455	0.560	0.442	0.642	0.523
$\gamma = 0.5$	0.751	0.437	0.570	0.428	0.651	0.510
$\gamma = 1$	0.876	0.421	0.580	0.416	0.661	0.497
$\gamma = 1.5$	0.869	0.705	0.690	0.663	0.671	0.585
			PSNR for fuzzy density/variance			
0.1/0.06	62.786	61.800	61.816	59.433	56.567	48.800
0.2/0.05	63.935	62.951	62.966	60.588	57.728	49.977
0.3/0.04	65.931	64.947	64.962	62.586	59.725	51.973
0.4/0.03	66.909	65.925	65.940	63.562	60.702	52.951
0.5/0.03	67.687	66.703	66.718	64.340	61.480	53.729

It is observed that for small size images the quality index improves considerably; on the other hand, when the image size is large the value of the quality index is comparable such that the visual quality improvement among larger size images does not vary much.

6 Conclusions

This study is related to the enhancement of overexposed and underexposed images using fuzzy logic. The fused image obtained using the proposed method provides significant contrast enhancement and visual information. The fused image obtained from the proposed fusion method is visually better than those obtained from DWT fusion, DWT with gamma enhancement, DWT with HE, adaptive HE and DC-FTR. Various objective image quality measures have been used to make a qualitative and quantitative comparison with other methods. Overall results show that the proposed method performs better than the other methods in terms of enhanced contrast, entropy, edge information reduced background noise. The proposed algorithm can be used for various ranges of applications, such as remote sensing, medical applications, etc. However, improvising the computational complexity with increasing membership function is one concern which can be taken up for future work. Although the computational time is comparable with the existing methods and in a nutshell, it is concluded that the proposed method gives convincing results in terms of qualitative and quantitative performance evaluation.

Table 3 Comparison of various performance metrics for different fusion methods for image set 3 (Cup)

	Proposed method	DC-FTR [14]	Adaptive HE [13]	DWT with HE [12]	DWT with GC [11]	DWT [10]
entropy	7.709	7.701	7.722	6.704	5.300	3.764
SD	65.835	65.913	66.031	61.174	62.011	74.354
AG	13.976	12.374	8.3768	8.5187	6.2855	6.026
FL	0.043	0.055	0.064	0.068	0.071	0.081
RGE	0.049	0.052	0.056	0.103	0.115	0.117
RMSE	17.932	18.575	21.660	23.612	23.777	26.699
A_C	0.966	0.965	0.883	0.891	0.847	0.884
time, s	9.612	9.658	9.803	9.705	9.848	8.984
			quality index, Q			
$\gamma = 0.2$	0.945	0.684	0.761	0.666	0.843	0.748
$\gamma = 0.4$	0.956	0.666	0.771	0.653	0.853	0.734
$\gamma = 0.5$	0.962	0.648	0.781	0.639	0.862	0.721
$\gamma = 1$	0.971	0.632	0.791	0.627	0.872	0.708
$\gamma = 1.5$	0.918	0.716	0.801	0.774	0.882	0.796
			PSNR for fuzzy density/variance			
0.1/0.06	61.790	60.804	60.820	58.437	55.571	47.804
0.2/0.05	62.939	61.955	61.970	59.592	56.732	48.981
0.3/0.04	64.935	63.951	63.966	61.590	58.729	50.977
0.4/0.03	65.913	64.929	64.944	62.566	59.706	51.955
0.5/0.03	66.691	65.707	65.722	63.344	60.484	52.733

Table 4 Comparison of various performance metrics for different fusion methods for image set 4 (Bridge)

	Proposed method	DC-FTR [14]	Adaptive HE [13]	DWT with HE [12]	DWT with GC [11]	DWT [10]
entropy	6.454	6.367	6.433	6.555	6.312	3.763
SD	64.545	64.923	66.031	76.496	69.027	62.361
AG	0.115	0.149	0.454	0.165	0.297	0.264
FL	0.015	0.019	0.022	0.070	0.082	0.084
RGE	0.930	0.930	0.887	0.913	0.891	0.901
RMSE	18.113	18.763	21.879	23.851	24.017	26.969
A_C	9.891	9.975	9.920	9.922	9.965	9.101
time, s	9.482	9.613	9.669	9.102	9.118	8.915
			quality index, Q			
$\gamma = 0.2$	0.952	0.694	0.770	0.677	0.850	0.757
$\gamma = 0.4$	0.963	0.677	0.779	0.663	0.859	0.743
$\gamma = 0.5$	0.969	0.659	0.789	0.650	0.869	0.730
$\gamma = 1$	0.978	0.643	0.799	0.638	0.879	0.718
$\gamma = 1.5$	0.917	0.727	0.809	0.784	0.889	0.803
			PSNR for fuzzy density/variance			
0.1/0.06	60.549	59.567	59.583	57.209	54.355	46.619
0.2/0.05	61.693	60.713	60.728	58.360	55.511	47.791
0.3/0.04	63.682	62.701	62.716	60.350	57.500	49.779
0.4/0.03	64.656	63.676	63.690	61.322	58.473	50.753
0.5/0.03	65.430	64.450	64.465	62.097	59.248	51.528

Table 5 Computational time in seconds for different membership functions using the proposed method

Number of membership functions	Image set 1	Image set 2	Image set 3	Image set 4
1	7.038	7.372	7.409	7.743
2	7.689	7.998	8.012	8.127
3	7.767	8.016	8.815	8.913
4	8.012	9.561	9.612	9.891

Table 6 Quality index for different regions of the fuzzy set taken

	Image set 1	Image set 2	Image set 3	Image set 4
$f_{\text{avg}}(i, j)$	0.782	0.611	0.822	0.829
$f_{\text{entropy}}(i, j)$	0.793	0.622	0.833	0.841
$f_{\text{edgeinfo}}(i, j)$	0.799	0.628	0.839	0.846
$f_{\text{bnoise}}(i, j)$	0.809	0.637	0.848	0.855
$f_{\text{img}}(i, j)$	0.889	0.846	0.857	0.964

Table 7 Quality Index of minimised values of $||f_{\text{img}}(i, j) - \mathfrak{r}||_{L^{-1}}$ for different values of λ

λ (image size)	Image set 1	Image set 2	Image set 3	Image set 4
0.2 (128 × 128)	0.782	0.731	0.768	0.713
0.4 (512 × 512)	0.891	0.841	0.861	0.898
0.6 (1024 × 1024)	0.892	0.839	0.861	0.892
0.8 (2048 × 2048)	0.894	0.842	0.868	0.894

7 References

[1] Goshtasby, A.A., Nikolov, S.: 'Advances in the state of art', *Inf. Fusion*, 2007, **8**, (2), pp. 114–118

[2] Yang, B., Jing, Z., Zhao, H.: 'Review of pixel level image fusion', *J. Shanghai Jiaotong Univ. (Sci.)*, 2010, **15**, (1), pp. 6–12

[3] Yuan, Y., Fang, J., Wang, Q.: 'Robust super pixel tracking via depth fusion', *IEEE Trans. Circuits Syst. Video Technol.*, 2014, **24**, (1), pp. 15–26

[4] Yang, H., Shao, L., Zheng, F., *et al.*: 'Recent advances and trends in visual tracking: a review', *Neurocomputing*, 2011, **74**, (18), pp. 3823–3831

[5] Wang, Q., Fang, J., Yuan, Y.: 'Multi-cue based tracking', *Neurocomputing*, 2014, **131**, (1), pp. 227–236

[6] Yang, B., Li, S.: 'Multifocus image fusion and restoration with sparse representation', *IEEE Trans. Instrum. Meas.*, 2010, **59**, (4), pp. 884–892

[7] Yang, C., Zhang, J.Q., Wang, X.R., *et al.*: 'A novel similarity based quality metric for image fusion', *Inf. Fusion*, 2008, **9**, (2), pp. 156–160

[8] Vu, C.T., Phan, T.D., Chandler, D.M.: 'S3: a spectral and spatial measure of local perceived sharpness in natural images', *IEEE Trans. Image Process.*, 2012, **21**, (3), pp. 934–945

[9] Petrović, V.: 'Subjective tests for image fusion evaluation and objective metric validation', *Inf. Fusion*, 2007, **8**, (2), pp. 208–216

[10] Yang, Y.: 'A novel DWT based multi-focus image fusion method', *Procedia Eng.*, 2011, **24**, pp. 117–181

[11] Suman, S., Hussin, F.A., Malik, A.S., *et al.*: 'Image enhancement using geometric mean filter and gamma correction for WCE images'. Neural Information Processing, November 2014 (LNCS, **8836**), pp. 276–283

[12] Cheng, H.D., Shi, X.J.: 'A simple and effective histogram equalization approach to image enhancement', *Digit. Signal Process.*, 2004, **14**, (2), pp. 158–170

[13] Huang, S.C., Cheng, F.C., Chiu, Y.S.: 'Efficient contrast enhancement using adaptive gamma correction with weighting distribution', *IEEE Trans. Image Process.*, 2013, **22**, (3), pp. 1032–1041

[14] Nandal, A., Rosales, H.G.: 'Enhanced image fusion using directional contrast rules in fuzzy transform domain', *SpringerPlus*, 2016, **5**, (1), p. 1846

[15] Perfilieva, I., Dankov, M.: 'Image fusion on the basis of fuzzy transforms'. World Scientific Proc. Series on Computer Engineering and Information Science, Computational Intelligence in Decision and Control, January 2008, vol. 1, pp. 471–476

[16] Dhingra, N., Nandal, A., Manchanda, M., *et al.*: 'Fusion of fuzzy enhanced overexposed and underexposed images', *Procedia Comput. Sci.*, 2015, **54**, pp. 738–745

[17] Zimmermann, H.J.: '*Fuzzy set theory and its applications*' (Kluwer Academic Publishers, 1991, 2nd edn.)

[18] Klir, J.G., Yuan, B.: '*Fuzzy set and fuzzy logic: theory and applications*' (Prentice Hall, 1995)

[19] Bezdek, J.C.: '*Pattern recognition with fuzzy objective function algorithms*' (Springer, 1981)

[20] Höppner, F., Klawonn, F., Kruse, R., *et al.*: '*Fuzzy cluster analysis: methods for classification, data analysis and image recognition*' (John Wiely & Sons, Chichester, 1999)

[21] Viattchenin, D.A.: '*A heuristic approach to possibilistic clustering: algorithms and applications*' (Springer-Verlag, Berlin, 2013)

[22] Jian-Lei, L., Jing-Xiu, Z., Bo, L.: 'A self-adaptable method of edge detection based on the gradient magnitude', *Optoelectron. Technol.*, 2007, **27**, (3), pp. 174–177

[23] Zhi, W., Sai-Xian, H.: 'An adaptive edge-detection method based on canny algorithm', *J. Image Graph.*, 2004, **9**, (8), pp. 957–962

[24] Barrenechea, E., Bustince, H., Beats, D.B., *et al.*: 'Construction of interval-valued fuzzy relations with application to the generation of fuzzy edge images', *IEEE Trans. Fuzzy Syst.*, 2011, **19**, (5), pp. 819–830

[25] Chen, S.M., Kao, P.Y.: 'TAIEX forecasting based on fuzzy time series, particle swarm optimization techniques and support vector machines', *Inf. Sci.*, 2013, **247**, pp. 62–71

[26] Roubos, H., Setnes, M.: 'Compact and transparent fuzzy models and classifiers through iterative complexity reduction', *IEEE Trans. Fuzzy Syst.*, 2001, **9**, (4), pp. 516–524

[27] An, G., Wu, J., Ruan, Q.: 'Independent Gabor analysis of multiscale total variation-based quotient image', *IEEE Signal Process. Lett.*, 2008, **15**, pp. 186–189

[28] Du, S., Ward, R.: 'Wavelet-based illumination normalization for face recognition'. IEEE Int. Conf. on Image Processing, Genova, Italy, September 2005

[29] Basri, R., Jacobs, D.: 'Lambertian reflectance and linear subspaces', *IEEE Trans. Pattern Anal. Mach. Intell.*, 2003, **25**, (2), pp. 218–233

[30] Horn, B.K.P.: '*Robot vision*' (MIT Press, Cambridge, MA, 1997)

[31] Goldfarb, D., Yin, W.: 'Parametric maximum flow algorithms for fast total variation minimization', *SIAM J. Sci. Comput.*, 2009, **31**, (5), pp. 3712–3743

[32] Available at http://imagefusion.org

[33] Choi, M.: 'A new intensity-hue-saturation fusion approach to image fusion with a tradeoff parameter', *IEEE Trans. Geosci. Remote Sens.*, 2006, **44**, (6), pp. 1672–1682

[34] Zheng, H., Zheng, D., Hu, Y., *et al.*: 'Study on the optimal parameters of image fusion based on wavelet transform', *J. Comput. Inf. Syst.*, 2010, **6**, (1), pp. 131–137

[35] Perez-Cruz, F., Navia-Vazquez, F., Figueiras-Vidal, A.R., *et al.*: 'Empirical risk minimization for support vector classifiers', *IEEE Trans. Neural Netw.*, 2003, **14**, (2), pp. 296–303

[36] Haghighat, M.B.A., Aghagolzadeh, A., Seyedarabi, H.: 'A non-reference image fusion metric based on mutual information of image features', *Comput. Electr. Eng.*, 2011, **37**, (5), pp. 744–756

[37] Wadud, M. A. A., Kabir, M. H., Dewan, M. A. A., *et al.*: 'A dynamic histogram equalization for image contrast enhancement', *IEEE Trans. Consum. Electron.*, 2007, **53**, (2), pp. 593–600

[38] Chen, Y., Xue, Z.Y., Blum, R.S.: 'Theoretical analysis of an information-based quality measure for image fusion', *Inf. Fusion*, 2008, **9**, (2), pp. 161–175

[39] Desale, R.P., Verma, S.V.: 'Study and analysis of PCA, DCT & DWT based image fusion techniques'. Int. Conf. on Signal Processing, Image Processing and Pattern Recognition, 7–8 February 2013, pp. 66–69

[40] Rahman, S.M.M., Ahmad, M.O., Swamy, M.N.S.: 'Contrast-based fusion of noisy images using discrete wavelet transform', *IET Image Process.*, 2010, **4**, (5), pp. 374–384

[41] Arivazhagan, S., Ganesan, L., Kumar, T.G.S.: 'A modified statistical approach for image fusion using wavelet transform', *Signal Image Video Process.*, 2009, **3**, (2), pp. 137–144

[42] Pajares, G., Cruz, J.M.: 'A wavelet-based image fusion tutorial', *J. Pattern Recognit.*, 2004, **37**, (8), pp. 1855–1872

[43] Kannan, K., Perumal, S.A., Arulmozhi, K.: 'Performance comparison of various levels of fusion of multi-focused images using wavelet transform', *Int. J. Comput. Applic.*, 2010, **1**, (6), pp. 71–78

[44] Ahmadvand, A., Daliri, M.R.: 'Invariant texture classification using a spatial filter bank in multi-resolution analysis', *Image Vis. Comput.*, 2016, **45**, pp. 1–10

[45] Perfilieva, I.: '*Fuzzy transforms, transactions on rough sets II. Fuzzy sets and rough sets*' (Springer-Verlag, Berlin, 2004), pp. 63–81, ISBN 3-540-23990-1

[46] Dvorak, A., Habiballa, H., Novak, V., *et al.*: 'The concept of LFLC 2000—its specificity, realization and power of applications', *Comput. Ind.*, 2003, **51**, pp. 269–280